JOURNAL OF SOLID STATE CHEMISTRY 32, 221–231 (1980)

The Elastic Strain Energy of Crystallographic Shear Planes in Reduced Tungsten Trioxide

E. IGUCHI* AND R. J. D. TILLEY†

Department of Metallurgical Engineering, Faculty of Engineering, Yokohama National University, Tokiwadai, Hodogaya-ku, Yokohama, 240 Japan; †School of Materials Science, University of Bradford, Bradford BD7 1DP, West Yorkshire, England

Received March 20, 1979

The elastic strain energy in reduced tungsten trioxide, which contains crystallographic shear (*CS*) planes, has been calculated using Fourier transform theory. This allows the effects of non nearest-neighbor *CS* planes to be evaluated, and also enables one to assess the relaxation energy of ions in the *CS* planes as well as the strain energy of the matrix between the *CS* planes. The results are presented for $\{10m\}$ $(2 \leq m \leq 7)$ and {001} *CS* plane types. They are compared with experimental data and also with the results of previous calculations using classical elasticity theory.

1. Introduction

Stoichiometric tungsten trioxide is built up of an infinite array of corner-sharing WO_6 octahedra. The crystal structure of tungsten trioxide is nearly cubic and when idealized is isostructural with the cubic ReO_3 (DO_9) structure (*1–3*). When tungsten trioxide is reduced to compositions down to approximately $WO_{2.85}$ or when certain lower valent metals are doped into tungsten trioxide, crystallographic shear (*CS*) planes are formed (*4–7*). If the degree of reduction is small, that is, from WO_3 to approximately $WO_{2.95}$, the *CS* planes lie upon {102} planes. As the degree of reduction increases, {103} *CS* planes are formed in preference to {102} (*4–7*). In tungsten trioxide doped with Nb and Ti, although the {102} and {103} *CS* sequence is adhered to, {001} *CS* planes seem to be favored and form in preference to extended {102} or {103} ranges. *CS* planes with indices between {103} and {001} also occur, particularly in the Nb_2O_5–WO_3 oxides, where well-ordered {104} *CS* phases have been recorded (*8–10*).

Anderson (*11*) suggested that strain energy may play a significant role in controlling the microstructure of *CS* phases. Following this, Stoneham and Durham (*12*) and Iguchi and Tilley (*13*, *14*) have calculated the strain energy due to *CS* planes in WO_3-like structures, but from different standpoints. Stoneham and Durham obtained the relaxation energy due to the interaction between defect forces in {001} *CS* planes, while Iguchi and Tilley computed the strain energy of ions in the matrix between *CS* planes. Stoneham and Durham employed, in their calculation, the Fourier transformation method which can be used for infinite ordered arrays and for pairs of *CS* planes. On the other hand, Iguchi and Tilley computed the strain energies using classical methods, which makes the calculations more complicated, but is compensated for as their

0022-4596/80/050221-11$02.00/0

treatment can be applied not only to ordered arrays but also to other plausible distributions of *CS* planes. It should be noted that the total strain energy is the sum of the relaxation energy which Stoneham and Durham obtained and the strain energy of the matrix which Iguchi and Tilley evaluated.

It would be desirable to estimate both the relaxation energy and the strain energy of the matrix by the same methods and compare the magnitudes of the energy terms involved. However, as the number of *CS* plane geometries is high the only practical way of making both these estimates is to use the compact and elegant Fourier transform method. However, the use of this technique presupposes that the whole of the crystal containing *CS* plane arrays can be treated as an elastic continuum. In a previous paper (*15*) the available experimental evidence was compared to the results of calculations for {001} *CS* planes to determine whether such an approximation was a reasonable one to make. The results suggested that the WO_3 lattice could be treated in this way, although the more ionic NbO_2F was not so suitable for Fourier transform methods.

Following this, we have obtained both the relaxation energy and the strain energy of ions caused by *CS* planes in reduced WO_3 in a way similar to that employed by Shimizu and Iguchi for TiO_2 (*16*). The results of these calculations are given here, and compared with experimental observations and results published previously.

2. Theory

The structures of WO_3 and the $\{10m\}$ *CS* phases have been fully described in the past and will not be reiterated here. In general when structural features need to be illustrated we will refer to {102} *CS* geometry unless, for reasons of clarity, other *CS* planes need to be shown. For completeness, we include in Fig. 1a an idealized representation of the WO_3 (ReO_3) structure, composed of

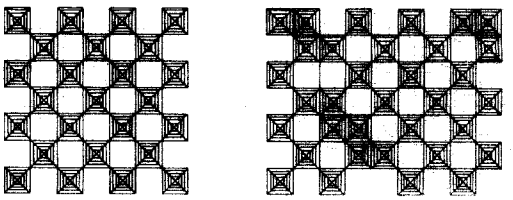

FIG. 1. Idealized representations of (a) WO_3; (b) $W_{15}O_{43}$, an oxide containing {103} *CS* planes.

corner-sharing MO_6 octahedra, and in Fig. 1b a {103} *CS* plane in a WO_3 matrix.

The strain energy, U, due to an infinite ordered array of $\{10m\}$ *CS* planes in an oxide of formula $W_nO_{3n-(m-1)}$ is written as follows (*16*):

$$U = U_S - U_R, \tag{1}$$

where U_R represents the relaxation energy of ions in the *CS* planes and U_S represents the strain energy of ions in the matrix due to forces arising in the *CS* planes. The calculation of U_S and U_R makes use of linear elasticity theory.

In order to simplify the calculations we have made a number of approximations. First we have assumed that the whole of the crystal, that is, both the *CS* planes and the regions between them, could be treated as an isotropic continuum, which allowed us to use the Fourier transform technique (*15*). In addition we have idealized the crystal structure of WO_3 to the cubic ReO_3 (DO_9) type, and assumed that the forces which cause the strain in the crystal are the same as those employed in our previous papers (*13–15*) and are short-range forces due to cation–cation intractions within the *CS* planes. To illustrate this, the forces supposed to be present in each unit of a {102} *CS* plane are shown in Fig. 2.

Long-range forces arising from all other ions in the lattice will also be present and have been considered by Dienes *et al.* (*17*) and Catlow (*18*) in other systems. To consider them here the physical properties of tungsten trioxide need to be known.

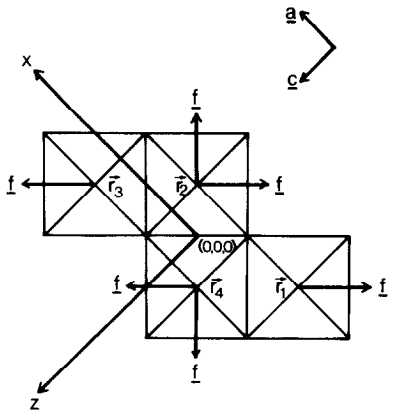

FIG. 2. Defect forces assumed to be present within a unit of a {102} *CS* plane. The cross in the center is the origin of the coordinates, *x*- and *z*-axes of which are indicated as well. The sites at which defect forces operate are represented with vectors $\mathbf{r}_1$, $\mathbf{r}_2$, $\mathbf{r}_3$, and $\mathbf{r}_4$.

Unfortunately, those that are needed have not yet been determined or reported. Therefore, we have assumed that the long-range forces are negligibly small.

For the purposes of the calculations we have chosen the origin of the coordinate axes to be in the center of a unit in a $\{10m\}$ *CS* plane and we have taken *x*-, *y*-, and *z*-axes parallel to the *a*-, *b*-, and *c*-crystal axes, respectively. In Fig. 3a we have illustrated this for a {102} *CS* plane. The periodic unit cell for an infinite ordered array of $\{10m\}$ *CS* planes in an oxide with formula $W_nO_{3n-(m-1)}$ can be constructed with vectors **A**, **B**, and $\mathbf{L}_n$, where

$$\begin{aligned} \mathbf{A} &= 4(m\mathbf{a}-\mathbf{c}), \\ \mathbf{B} &= 2\mathbf{b}, \\ \mathbf{L}_n &= 2(2n-2m+1)\mathbf{a}+2\mathbf{c}. \end{aligned} \tag{2}$$

In these equations, the primitive translation vectors of the WO_3 lattice, **a**, **b**, **c**, are

$$\begin{aligned} \mathbf{a} &= (a/4)\mathbf{i}, \\ \mathbf{b} &= (a/2)\mathbf{j}, \\ \mathbf{c} &= (a/4)\mathbf{k}, \end{aligned} \tag{3}$$

where *a* is the lattice constant, and **i**, **j**, and **k** indicate the unit vectors along the *x*-, *y*-, and *z*-axes. The structure of an infinite ordered array of *CS* planes can be constructed by the formal geometrical translation **T**, given by

$$\mathbf{T} = n_1\mathbf{A} + n_2\mathbf{B} + n_3\mathbf{L}_n, \tag{4}$$

where n_1, n_2, and n_3 are integers.

The homologous series of oxides which have ordered arrays of {001} *CS* planes are represented by the formula W_nO_{3n-1}. This series can be treated in the same way to other homologous series except the vectors **A**, **B**, and $\mathbf{L}_n$ which have the following form, as indicated in Fig. 3b:

$$\begin{aligned} \mathbf{A} &= 4\mathbf{a}, \\ \mathbf{B} &= 2\mathbf{b}, \\ \mathbf{L}_n &= -2\mathbf{a}-2(2n-1)\mathbf{c}. \end{aligned} \tag{2'}$$

The energy terms U_S and U_R have been obtained in a way similar to the calculations in rutile (*16*). Following this procedure the relaxation energy, U_R, is written as a sum over the first Brillouin zone of the lattice.

$$U_R = (1/N)\sum_{\mathbf{r}}\sum_{\alpha} F_\alpha(\mathbf{r})\sum_{\mathbf{q}}\sum_{\beta} \times e^{-i\mathbf{qr}}\tilde{G}_{\alpha\beta}(\mathbf{q})\tilde{F}_\beta(\mathbf{q}), \tag{5}$$

where *N* is the number of the unit cells, $F_\alpha(\mathbf{r})$ represents the αth component of the defect force at **r**, $\tilde{F}_\beta(\mathbf{q})$ is the βth component of the Fourier transformed force, $\tilde{G}_{\alpha\beta}(\mathbf{q})$ denotes the $\alpha\beta$th component of the Fourier transformed Green's function, $\sum_\alpha$ or $\sum_\beta$ indicates the summation of every component of the defect force, and $\sum_{\mathbf{r}}$ means the summation of the relaxation energies of all ions in the cell.

The strain energy of ions in the periodic unit, U_S, is assumed to be expressed as follows:

$$U_S = \sum_{\mathbf{r}} (4\pi r_{\mathbf{r}}^3/3)w(\mathbf{r}), \tag{6}$$

where $\sum_{\mathbf{r}}$ has a meaning similar to that in Eq. (5), and $w(\mathbf{r})$ represents the strain energy density of the ion at **r**, the ionic radius of this

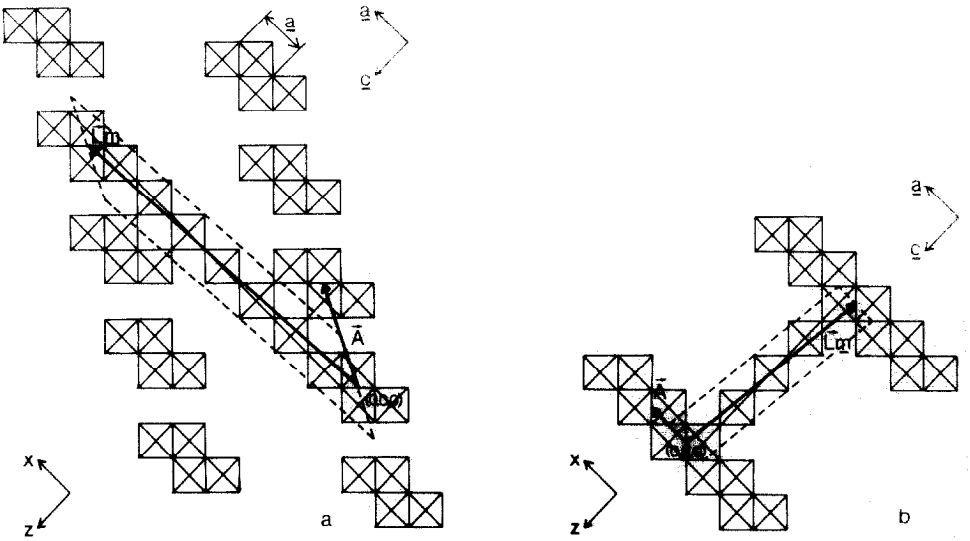

FIG. 3. The idealized structures of (a) W_9O_{26}, an oxide containing {102} *CS* planes; (b) W_5O_{14}, an oxide containing {001} *CS* planes. The broken lines represent the periodic unit cells. The vectors, $\mathbf{A}, \mathbf{L}_n$, lie upon the {010} plane and the vector **B** is normal to the {010} plane. The lattice constant a and the crystal axes a, c are also indicated.

ion being abbreviated as $r_\mathbf{r}$. As linear elastic theory is used, the unit cell volume should be used theoretically instead of the ionic volume in Eq. (6). The tungsten trioxide structure, however, consists of edge-shared WO_6 octahedra as shown in Fig. 1 and has chains of voids. The volume of the voids is nearly equal to the volume of ions. Thus, in order to prevent overestimation of the strain energy of ions, we have made the assumption represented in Eq. (6). The strain energy density for a cubic elastic continuum has the form (*19*)

$$w = \tfrac{1}{2}C_{11}\sum_{i=1}^{3} e_{ii}^2 + C_{12}\sum_{i,j=1}^{3} e_{ii}e_{jj} + 2C_{44}\sum_{i,j=1}^{3} e_{ij}^2 \quad (i \neq j), \tag{7}$$

where the klth component of the strain at $\mathbf{r}$, $e_{kl}(\mathbf{r})$, is given by the use of the Fourier transformation as follows:

$$e_{kl}(\mathbf{r}) = -(i/2\mathrm{N})\sum_{\mathbf{q}} e^{i\mathbf{qr}} \sum_{\beta} [q_l \tilde{G}_{k\beta}(\mathbf{q}) + q_k \tilde{G}_{l\beta}(\mathbf{q})]\tilde{F}_\beta(\mathbf{q}), \tag{8}$$

where q_l is the lth component of the wave vector $\mathbf{q}$ and every other notation has the same meaning as in Eq. (5).

The forces in the infinite ordered array repeat under the translation **T** and all transforms $\tilde{F}(\mathbf{q})$ vanish unless $\mathbf{q}$ reflects this transformation. Then each component of wave vector $\mathbf{q}$ can be written as

$$\begin{aligned} &\mathbf{q} = (q_x, q_y, q_z), \\ &q_x = [2\pi/(2n-m+1)a](H+2M), \\ &q_y = (2\pi/a)J, \\ &q_z = [2\pi/(2n-m+1)a]\times \\ &\qquad [-(2n-2m+1)H + 2mM], \end{aligned} \tag{9}$$

where H, J, and M are integers.

The strain energy of the ions and the relaxation energy can be obtained as a sum over discrete values of $\mathbf{q}$ in the first Brillouin zone of the lattice, i.e., $-(4\pi/a) \leqq q_x, q_z < (4\pi/a)$ and $-(2\pi/a) \leqq q_y < (2\pi/a)$.

The Fourier transformed Green's function for a cubic elastic continuum is given

as (*20*)

$$C_{44}\tilde{G}_{ij}(\mathbf{q}) = (1/q^2) \times\left(\Lambda_i\delta_{ij} - \Lambda_i\Lambda_j\frac{\gamma K_i K_j}{1+\gamma\sum_{l=1,3-l}K_l^2}\right), \quad (10)$$

where the K_i are the direct cosines (q_i/q) of $\mathbf{q}$ and

$$\Lambda_i(\mathbf{q}) = (1+\delta K_i^2)^{-1}. \quad (11)$$

The dimensionless factors depend only on the elastic constants, C_{ij},

$$\gamma = (C_{12}+C_{44})/C_{44}, \qquad \delta = (C_{11}-C_{12}-2C_{44})/C_{44}. \quad (12)$$

As the elastic constants of WO_3 have not yet been determined, we have used the same ratios of the elastic constants as in our previous papers (*13, 14*), viz.,

$$C_{11}:C_{12}:C_{44} = 16:7:5. \quad (13)$$

As shown in Fig. 2, one unit in a $\{10m\}$ *CS* plane has $2m$ cations at which the forces operate. We have taken the vectors to those cations from the origin, $\mathbf{r}_1, \mathbf{r}_2, \ldots, \mathbf{r}_{2m}$, as shown in Fig. 2. In the case of the {102} *CS* plane, the forces and the sites at which they operate are

site $\mathbf{r}$	force $F(\mathbf{r})$
$\mathbf{r}_1, (-3a/4, 0, -a/4)$	$f/2^{1/2}(-1, 0, -1)$
$\mathbf{r}_2, (a/4, 0, -a/4)$	$f/2^{1/2}(0, 0, -2)$
$\mathbf{r}_3, (3a/4, 0, a/4)$	$f/2^{1/2}(1, 0, 1)$
$\mathbf{r}_4, (-a/4, 0, a/4)$	$f/2^{1/2}(0, 0, 2)$

The defect forces and sites in other $\{10m\}$ *CS* planes are quite similar to those in the {102} case and, then, the following relations are obtained:

$$\mathbf{r}_i = -\mathbf{r}_{i+m}, \qquad F(\mathbf{r}_i) = -F(\mathbf{r}_{i+m}) \quad (i \leq m). \quad (14)$$

The Fourier transformed $\tilde{F}(\mathbf{q})$ is then given as

$$\tilde{F}_\beta(\mathbf{q}) = \sum_{\mathbf{r}} F_\beta(\mathbf{r})\, e^{i\mathbf{q}\mathbf{r}} = 2i\sum_{\mathbf{r}=\mathbf{r}_1}^{\mathbf{r}_m} F_\beta(\mathbf{r}_i)\sin(\mathbf{q}\mathbf{r}_i), \quad (15)$$

where $\sum_{\mathbf{r}=\mathbf{r}_1}^{\mathbf{r}_m}$ indicates summation over the sites at which the defect forces act. The following ionic radii for O^{2-} and W^{6+}, r_0 and r_W, were used in this calculation: $r_0 = 1.40$ Å, $r_W = 0.60$ Å (*21*).

3. Results and Discussion

As in our previous papers we have attempted to calculate the elastic strain energy of crystals containing *CS* planes. We then assumed that the favored microstructures in real crystals would be those corresponding to the smallest strain energy. A comparison of the results with experimental observations on crystals containing *CS* structures showed that good agreement existed when the relaxation energy of the ions was ignored. In the results and discussion that follow we have repeated this procedure, but have also calculated the relaxation energy as well. We have therefore treated the same situations as before, that is, the stability of isolated *CS* planes, the relative stability of arrays of various $\{10m\}$ *CS* planes, and the relative stability of homologs within a series of oxides based on one *CS* plane type.

A. The Strain Energy per Unit Area per CS Plane

First we have calculated the strain energy and the relaxation energy per unit area per *CS* plane for crystals with formulas $W_nO_{3n-(m-1)}$ $(2 \leq m \leq 7)$ and W_nO_{3n-1} ($\{001\}$ *CS* planes), $(U_S)_A$ and $(U_R)_A$, respectively, and plotted them as a function of n in Figs. 4 and 5. The vertical axes of these figures are plotted in units of $[(f/\pi)^2/C_{44}]/[L]^3$.[1]

[1] In this report we have calculated the strain energy per unit area per plane in units of $[(f/\pi)^2/C_{44}]/[L]^3$ and the strain energy per unit volume in units of $[(f/\pi)^2/C_{44}a]/[L]^3$, where $[L]$ represents the dimension of length. Therefore, if f and C_{44} are represented in units of (eV/Å) and (eV/Å^3), respectively, $[L]$ will be in units of (Å). Then $[(f/\pi)^2/C_{44}]/[L]^3$ is represented in units (eV/Å^2) and $[(f/\pi)^2/C_{44}a]/[L]^3$ in units of (eV/Å^3).

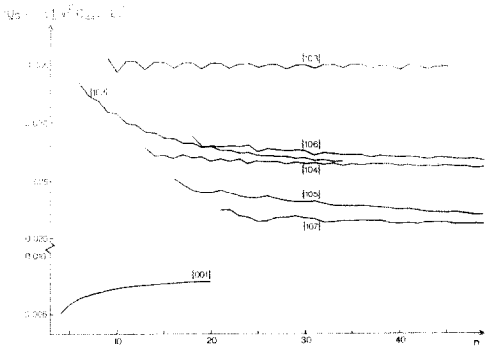

FIG. 4. The strain energy of ions per unit area per plane, $(U_S)_A$ vs n in $W_nO_{3n-(m-1)}$. The vertical axis on the left-hand side represents units of $(f/\pi)/C_{44}/[L]^3$.

The $(U_S)_A$ curves are seen to be oscillatory, i.e., they have series of peaks and valleys with a periodicity of $\Delta n = m$, except the {001} case. This behavior is the same as that found previously using classical methods of evaluating the strain energy of ions in the matrix between *CS* planes and is due to the relative dispositions of the *CS* planes in the array (*14*). Apart from this feature, the strain energy per unit area can be seen to be relatively constant, apart from the lowest n value region.

In our previous papers, we could not evaluate the strain energy within *CS* planes, and so we treated this term as an unknown parameter, U_{self} (*13*). This term consists of the relaxation energy due to the interaction between forces in one *CS* plane and the strain energy of ions within this *CS* plane caused by the forces in this plane. In the theoretical treatment used here, the strain energy of ions within one *CS* plane, one part of U_{self}, is included in $(U_S)_A$. This term is an eigenvalue, being independent of the surrounding *CS* planes. Therefore, the fact that no general increase of $(U_S)_A$ with increasing n is observed indicates that the strain energy within one *CS* plane plays a dominant role in $(U_S)_A$.

Unlike $(U_S)_A$ the values of $(U_R)_A$ are always found to be negative. This may be due to the fact that each cation in a *CS* plane is attracted to the inside of the *CS* plane by other forces in that *CS* plane. This result coincides with that in reduced rutile (*16*) and may be a general property of *CS* planes. As shown in the figures, the relaxation energy is larger than the strain energy of the ions and should play an important role in controlling the microstructures of *CS* phases in those situations where the *CS* plane itself can be regarded as an isotropic continuum.

In Fig. 6, the total energy U_A, the summation of $(U_S)_A$ and $-(U_R)_A$, has been plotted as a function of n. The striking feature is that U_A is smallest for {001} *CS*, and then we pass through a series, with {102} being the next lowest, and so on. Although we have not included relaxation energy in our previous calculations, these new results are still in close accord with the earlier sequence, and

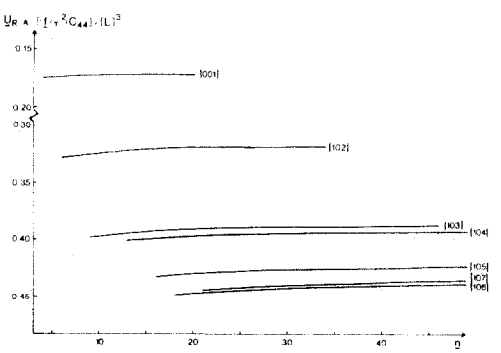

FIG. 5. The relaxation energy per unit area per plane, $(U_R)_A$, as a function of the n value.

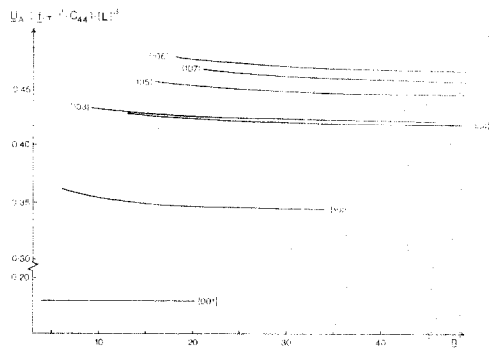

FIG. 6. The strain energy per unit area per plane, U_A, vs n, where $U_A = (U_S)_A - (U_R)_A$.

reemphasize that in terms of strain energy, {001} *CS* planes should always be the most favored.

A second point to note is that U_A decreases as n increases in each case. The variation of U_A with change of n is, however, small, which means that surrounding *CS* planes in the ordered array contribute only slightly to U_A compared with U_{self}, i.e., the contribution from the *CS* plane in which we have chosen the origin of the coordinates as described before. This result is important, as it shows that neglect of nearest-neighbor *CS* planes is not so important. Thus, in cases where *CS* planes cannot be treated as isotropic continua and where Fourier transformation techniques cannot be used, the results obtained by classical analysis are reliable.

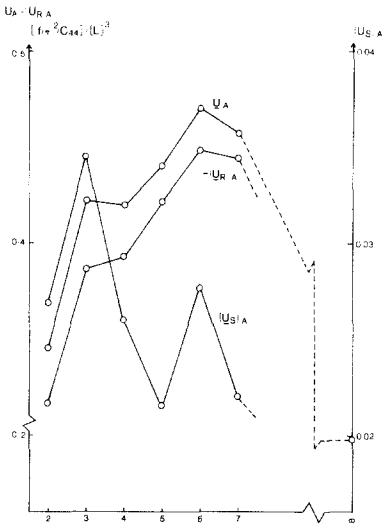

FIG. 7. The energy terms per unit area per plane, ${}^0U_A$, ${}^0(U_S)_A$, and $-{}^0(U_R)_A$, which are obtained by extrapolating each term to $n = \infty$ in Figs. 5 and 6, are plotted as a function of m.

B. Isolated CS Planes

The result in Fig. 6 suggests that the U_A value in every case will tend to some constant value at high n value, which means that the U_A values at $n = \infty$ are insensitive to the interactions due to surrounding *CS* planes. If an isolated *CS* plane is introduced into a single crystal, the increase in energy per unit area of the *CS* plane should be equivalent to the U_A value extrapolated to $n = \infty$ in Fig. 6. In Fig. 7 we have plotted ${}^0U_A$, ${}^0(U_S)_A$, and $-{}^0(U_R)_A$ as a function of m, which are obtained by extrapolating U_A, $(U_S)_A$, and $-(U_R)_A$ to $n = \infty$ in Fig. 6.

As the relaxation energy is the largest component of the strain energy, the behavior of ${}^0U_A$ is quite similar to that of $-{}^0(U_R)_A$. It is found that the ${}^0U_A$ curve has a peak at $m = 3$ to 4, the maximum at $m = 6$ to 7, and a valley at $m = 4$ to 5, and the U_A value is then likely to decrease smoothly to {001} ($m = \infty$) as m increases beyond $m = 7$.

${}^0(U_S)_A$ decreases as m increases but this curve has a pronounced series of peaks and valleys. In our previous report (*14*), the strain energy of ions in the matrix between *CS* planes extrapolated at $n = \infty$ had a maximum at $m = 3$–4 but decreased smoothly as m increased beyond $m = 4$. The result in this report, therefore, coincides with our previous result in the fact that the strain energy of ions extrapolated at $n = \infty$ has a peak at $m = 3$–4, but the series of peaks and valleys which appears in this study are rather different. The reason for this is that here we also include the strain energy of the ions in the *CS* plane themselves, U_{self}, and not just those between *CS* planes, as in the past. Unfortunately we cannot use this result to determine how well the Fourier transform method applies to WO_3 as the observations must be related to the overall curve ${}^0U_A$, which, as we have pointed out, has a form similar to that observed from our more classical analysis.

The overall shape of the U_A curve is similar to that presented before, and the same overall conclusion holds. It is once again found that the increase in strain energy when an isolated *CS* plane is introduced into a crystal is smallest for an {001} *CS* plane and then, apart from high m values which we

have not calculated, the sequence is $\{102\} < \{103\} < \{104\}$ and so on, as shown in Fig. 7. This result reemphasizes the fact that the elastic strain energy alone does not control the formation of isolated *CS* planes in slightly reduced oxides with the ReO_3 structure. The various factors which also contribute to the formation energy of isolated *CS* planes have been dealt with in detail previously (*14*, *22*) and will not be considered further here.

C. The Strain Energy of an Ordered Array of CS Planes

In Fig. 8, we have plotted the strain energy per unit volume of oxide, $W_nO_{3n-(m-1)}$, containing an ordered array of $\{10m\}$ *CS* planes as a function of the composition, x in WO_x. The strain energy per unit volume, U_V, decreases to zero as x increases to 3.0 (the perfect crystal) and every curve of U_V vs x is almost linear. At any composition x, the elastic strain energy is lowest for $\{001\}$ *CS* planes and highest for $\{102\}$ *CS* planes, and U_V decreases as m in $\{10m\}$ increases. This result agrees with the results obtained in our previous paper (*14*) which employed a quite different model for *CS* planes. It can be seen that there is no crossover in energy curves, while in reduced rutile in which a similar model for *CS* planes was used, two energy curves intersect each other (*16*).

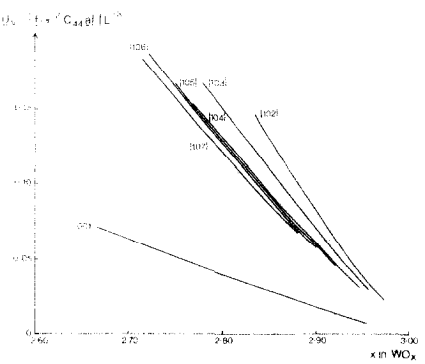

FIG. 8. The strain energy U_V per unit volume in infinite ordered arrays of $\{10m\}$ *CS* planes ($m = 2-7, \infty$) as a function of the composition, x in WO_x.

Experimentally, isolated or paired $\{102\}$ *CS* planes are formed initially during the preparation of samples which consist predominantly of WO_3. As the heating time is prolonged or if reduction conditions allow it, the density of *CS* planes increases and the ordered arrays may be formed. As the strain energy of well-ordered $\{102\}$ arrays has the largest value, one would expect these arrays to change to arrays with a higher m value and a smaller overall strain energy. According to Fig. 8, the transition from well-ordered $\{102\}$ arrays to the most stable $\{001\}$ arrays will be the one giving the greatest gain in energy.

As we have pointed out before (*14*) how this process will proceed is a question of mechanism and will particularly involve whether the reaction takes place totally in the solid or by way of vapor intermediates. We can, though, consider the relative stabilities of crystals containing arrays of *CS* planes. In general, if we have a crystal containing an ordered array of $\{10m\}$ *CS* planes, it can disproportionate to two arrays, one on $\{10(m+1)\}$ planes and one on $\{10(m-1)\}$ planes. If this process results in a gain in strain energy we can regard the $\{10m\}$ array as stable while if the total strain energy after the hypothetical transformation is less than before we can regard the $\{10m\}$ array to be less stable than the pair of arrays $\{10(m+1)\}$ and $\{10(m-1)\}$. Hence if $U_V(m) < \{U_V(m+1) + U_V(m-1)\}/2$, at some composition the $\{10m\}$ ordered array is stable at this composition, where $U_V(m)$ represents the strain energy of an oxide of the formula $W_nO_{3n-(m-1)}$ containing the $\{10m\}$ ordered array, and $U_V(m+1)$ or $U_V(m-1)$ indicates the strain energy of an oxide of the formula $W_{n_1}O_{3n_1-m}$ containing the $\{10, m+1\}$ arrays or that of an oxide of $W_{n_2}3n_2-(m-2)$ containing the $\{10, m-1\}$ arrays. On the other hand, if $U_V(m) > \{U_V(m+1) + U_V(m-1)\}/2$, the $\{10m\}$ array is unstable and this phase would not be formed.

There are a number of ways to present these data but we have chosen to do this

graphically, and for a composition of $x = 2.85$. If we plot the strain energy values at the bottom of sharp-bladed curves of the sort postulated for the free energy variation with composition of *CS* phases (*11*) then we can use the common tangent rule to see which of the various $\{10m\}$ arrays are stable relative to their neighbors. The result is shown in Fig. 9, which shows that the {103} array and {104} arrays are stable, but, as the {001} array is the most stable phase, they are, in the strict sense, metastable. The $\{10m\}$ arrays in which $m \geqq 5$ are not even metastable phases. Therefore our results suggest that in the progression from {102} *CS* phases to the ordered {001} phases, the metastable {103} and {104} materials will also be observed experimentally. This prediction is in good agreement with the cases with Nb and Ti. Recently, in the Nb_2O_3–WO_3 system, the {104} ordered arrays observed to form in this oxide after heating for 2 or 3 days disappeared and well-ordered {001} *CS* planes replaced them on heating to obtain thermal equilibrium state (Tilley, unpublished data). This experimental result agrees very well without our calculations. It is to be expected,

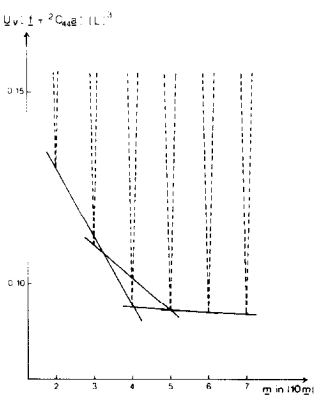

FIG. 9. The strain energy per unit volume in infinite ordered *CS* arrays as a function of m in $\{10m\}$ at the composition of $x = 2.85$. It is found that $U_V(3) < (U_V(2) + U_V(4))/2$ and $U_V(4) < (U_V(3) + U_V(5))/2$, while $U_V(m) \geqslant (U_V(m-1) + U_V(m+1))/2$ $(m \geqslant 5)$, where $U_V(m)$ is the strain energy per unit volume of the infinite ordered $\{10m\}$ array at $x = 2.85$.

though, that temperature will have a profound effect on the stability of these phases, and higher temperatures may shift the position of stability to other homologs in the series.

D. Stability of the Homologous Oxides in a {10m} Array

In our preceding publications we have calculated the relative stabilities of the members of several of the possible homologous series of oxides $W_nO_{3n-(m-1)}$ (*16*). It is therefore desirable to repeat the calculations here to compare the predictions of the Fourier transform method with that of the classical method used earlier. The technique is straightforward mathematically.

Imagine a crystal of the oxide $W_nO_{3n-(m-1)}$ containing an ordered array of $\{10m\}$ *CS* planes. Simply by redistributing the *CS* planes laterally, we can formally convert the original crystal into a crystal which contains two phases, $W_{n_1}O_{3n_1-(m-1)}$ and $W_{n_2}O_{3n_2-(m-1)}$, distributed alternately without changing the total number of *CS* planes, that is,

$$2W_nO_{3n-(m-1)} = W_{n_1}O_{3n_1-(m-1)} + W_{n_2}O_{3n_2-(m-1)}. \qquad (16)$$

Though there are a number of combinations of n_1 and n_2 which are subject to the condition of Eq. (16), we have employed the couple $n_1 = n-1$ and $n_2 = n+1$. The theoretical treatment is the same as for an infinite ordered array except that we have chosen the origin of the coordinates in the "two-phase" mixture to be midway along the vector **D**, from the origin of the unit cell of $W_{(n-1)}O_{3(n-1)-(m-1)}$ to that of $W_{(n+1)}O_{3(n+1)-(m-1)}$. This is illustrated for the case of {102} *CS* planes in Fig. 10. It is important to note the structure of this array carefully. In the Fourier transform method it is vital to employ a periodic structure. In our case it forces us to consider not a subdivision of the crystal into two separate parts, one of

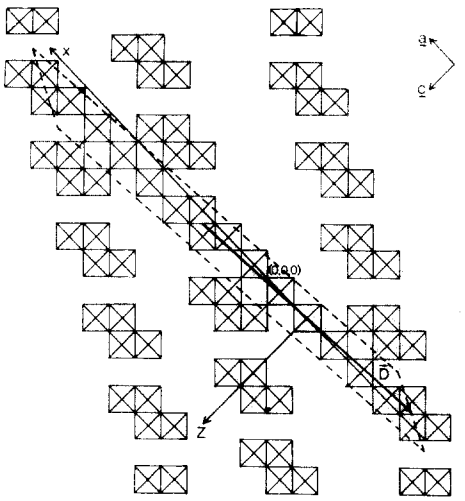

FIG. 10. A crystal containing two phases, W_7O_{20} and W_9O_{26}, based upon {102} *CS*. The periodic unit cell is the "two-phase" mixture is indicated by broken lines. The origin of the coordinates in the "two-phase" mixture is taken to be midway along the vector **D** from the origin of the W_7O_{20} unit cell to the origin of the W_9O_{26} unit cell.

which is the $(n-1)$ homologue and one of which is the $(n+1)$ homologue, but into a crystal which consists of a totally ordered array of alternating $(n-1)$ and $(n+1)$ slabs.

The Fourier transformed defect force of the "two-phase" mixture, $\tilde{F}_{\text{mix}}(\mathbf{q})$, has the form

$$\tilde{F}_{\text{mix}}(\mathbf{q}) = \sum_{\mathbf{r}-\mathbf{D}/2} F(\mathbf{r}-\mathbf{D}/2)\, e^{i\mathbf{q}(\mathbf{r}-\mathbf{D}/2)} + \sum_{\mathbf{r}+\mathbf{D}/2} F(\mathbf{r}+\mathbf{D}/2)\, e^{i\mathbf{q}(\mathbf{r}+\mathbf{D}/2)} = 2\cos(\mathbf{qD}/2)\tilde{F}(\mathbf{q}), \quad (17)$$

where the vector **D** has the form

$$\mathbf{D} = 2(2n-2m-1)\mathbf{a}+2\mathbf{c} \quad \text{for } \{10m\},$$
$$\mathbf{D} = -2\mathbf{a}-2(2n-3)\mathbf{c} \quad \text{for } \{001\}. \quad (18)$$

The vector $\mathbf{L}_n$ in Eq. (4) is replaced by the vector $\mathbf{L}_{\text{mix}}$ shown as follows:

$$\mathbf{L}_{\text{mix}} = \mathbf{L}_{n-1} + \mathbf{L}_{n+1} = 2\mathbf{L}_n. \quad (19)$$

Using these relations, we have calculated the energy per unit volume of the "two-phase" mixture which is denoted as U_{mix}. The difference in energy per unit volume, $\Delta U_n = U_n - U_{\text{mix}}$, is easily obtained as a function of n for the cases of interest. If ΔU_n is positive, the oxide $W_nO_{3n-(m-1)}$ has a higher overall elastic strain energy, and the sample would gain by disproportionation into the ordered array of alternating $(n-1)$ and $(n+1)$ lamellae. If ΔU_n is negative, disproportionation would increase the strain energy in the system and disproportionation is less likely.

For {102}, {103}, and {001} arrays, the results show that disproportionation into an ordered array will not usually take place if a lowering of elastic strain is the factor of prime importance. This is not surprising, as no such ordered arrays have ever been found experimentally, and other factors, such as entropy, will have a significant contribution to make to the energy of an ordered system. However, in a few cases it was found that such a disproportion was favorable in terms of elastic strain, and if the elastic strain terms dominate, such ordered $(n+1)+(n-1)$ arrays could possibly form. Although these have not been observed in the *CS* phases, they have been found in some of the intergrowth tungsten bronze phases recently reported, notably in the Sn_xWO_3 and Pb_xWO_3 systems (*23*).

E. Conclusions

In our previous work (*13*, *14*) the matrix between *CS* planes is assumed to be an isotropic continuum and the defect forces from surrounding *CS* planes cannot pass through a *CS* plane at all. On the other hand, in this report, not only the matrix between *CS* planes but also the regions of *CS* planes are treated as isotropic continua and the defect forces can pass through *CS* planes without any damping. In spite of the difference between these two models, most of the results in this report are similar to the results

in our previous work. Therefore, one cannot conclude which model is better. In order to clarify this point, we have to establish a correlation between the theory and the experimental observations in more detail. To do this it is important to consider situations much closer to equilibrium. To this end, *CS* phases heated for periods of time of several months are needed. The results of such studies will be reported in the future.

Acknowledgments

The authors are indebted to Professor J. S. Anderson for useful discussions and E.I. is indebted to Professor R. Wada for his encouragement during this work.

References

1. S. TANISAKI, *J. Phys. Soc. Japan* **15**, 566, 573 (1960).
2. B. O. LOOPSTRA AND P. BOLDRINI, *Acta Crystallogr.* **21**, 158 (1966); B. O. LOOPSTRA AND H. M. RIETVELD, *Acta Crystallogr. Sect. B* **25**, 1420 (1969).
3. E. SALJE AND K. VISWANATHAN, *Acta Crystallogr. Sect. A* **31**, 356 (1975).
4. J. S. ANDERSON, in "Surface and Defect Properties of Solids" (J. M. Thomas and M. W. Roberts, Eds.), Vol. 1, pp. 1–53, The Chemical Society, London (1972).
5. J. S. ANDERSON AND R. J. D. TILLEY, *in* "Surface and Defect Properties of Solids," (J. M. Thomas and M. W. Roberts, Eds.), Vol. 3, pp. 1–56, The Chemical Society, London (1974).
6. R. J. D. TILLEY, *in* "MTP International Review of Science: Inorganic Chemistry" (L. E. J. Roberts, Ed.), Ser. 1, Vol. 10, pp. 279–313, Butterworths, London (1972).
7. R. J. D. TILLEY, *in* "MTP International Review of Science: Inorganic Chemistry" (L. E. J. Roberts, Ed.), Ser. 2, Vol. 10, pp. 73–110, Butterworths, London (1972).
8. J. G. ALLPRESS, *J. Solid State Chem.* **4**, 173 (1972).
9. L. A. BURSILL AND B. G. HYDE, *J. Solid State Chem.* **4**, 430 (1972).
10. T. EKSTRÖM AND R. J. D. TILLEY, *Mater. Res. Bull.* **9**, 705 (1974).
11. J. S. ANDERSON, *in* "The Chemistry of Extended Defects in Non-Metallic Solids" (L. Eyring and M. O'Keeffe, Eds.), p. 14, North-Holland, Amsterdam (1970).
12. A. M. STONEHAM AND P. J. DURHAM, *J. Phys. Chem. Solids* **34**, 2127 (1973).
13. E. IGUCHI AND R. J. D. TILLEY, *Phil. Trans. Roy. Soc. London Ser. A* **286**, 55 (1977).
14. E. IGUCHI AND R. J. D. TILLEY, *J. Solid State Chem.* **18**, 121, 131 (1978).
15. E. IGUCHI AND R. J. D. TILLEY, *J. Solid State Chem.* **29**, 435 (1979).
16. Y. SHIMIZU AND E. IGUCHI, *Phys. Rev. B* **17**, 2505 (1978).
17. G. J. DIENES, D. O. WELCH, C. R. FISCHER, R. D. HATCHER, O. LAZARETH, AND M. SAMBERG, *Phys. Rev. B* **11**, 3060 (1975).
18. C. R. A. CATLOW, *Proc. Roy. Soc. London Ser. A* **353**, 533 (1977).
19. H. B. HUNTINGTON, *in* "Solid State Physics" (H. Ehrenreich, F. Seitz, and D. Turnbull, Eds.), Vol. 17, 216, Academic Press, New York (1965).
20. P. H. DEDERICHS AND G. LEIBRIED, *Phys. Rev.* **188**, 1175 (1969).
21. R. D. SHANNON AND G. T. PREWITT, *Acta Crystallogr. Sect. B* **25**, 925 (1969).
22. R. J. D. TILLEY, *J. Solid State Chem.* **19**, 53 (1976).
23. T. EKSTRÖM, M. PARMENTIER, AND R. J. D. TILLEY, submitted for publication.